Static electric polarizabilities of sodium clusters

I. Moullet*
Institut de Physique Expérimentale, Ecole Polytechnique Fédérale de Lausanne, CH-1015 Lausanne, Switzerland

José Luís Martins
Department of Chemical Engineering and Materials Science, University of Minnesota, Minneapolis, Minnesota 55455

F. Reuse and Jean Buttet
Institut de Physique Expérimentale, Ecole Polytechnique Fédérale de Lausanne, CH-1015 Lausanne, Switzerland
(Received 9 July 1990; revised manuscript received 10 September 1990)

We present pseudopotential local-spin-density calculations of the static electric polarizabilities of sodium clusters up to nine atoms. We show that the comparison of the calculated polarizabilities with the experimental average polarizabilities and with the observed collective resonance frequencies gives information on which isomer is most probably observed in the experiments. Our results indicate that the plateau in the observed polarizability between Na_6 and Na_7 could be related to the change from two-dimensional to three-dimensional geometries. We also present calculations for the permanent dipole moment of the clusters, and evaluate the effects of the ionic vibrations on the molecular polarizability of Na_2 and Na_3.

I. INTRODUCTION

Clusters have properties that are different from those of the bulk material, in particular their geometrical structure may be quite different from that of bulk-phase fragments. Although the geometrical structure of a cluster can be argued to be its most fundamental property, the experimental evidence on the structure of very small clusters is scarce, constituting one of the major difficulties in our understanding of these fascinating materials. In this context theorists must either guess or predict cluster geometries before they can calculate their properties, and theoretical calculations have been a major source of suggestions for cluster geometries. However, metal clusters often have several isomers with similar energies, and the accuracy of the calculations may not be sufficient to determine which one is the most stable isomer. The measurement of properties that are sensitive to the geometry and which could distinguish between isomers that are close in energy is very important in establishing the reliability of the theoretical predictions.

The static electric polarizability of clusters is a very interesting property, not only because it probes the response to a simple perturbation, but also because the polarizability is expected to be sensitive to the cluster shape. The average static electric polarizability of sodium clusters with up to 40 atoms was measured by Knight *et al.*[1] from the deflection of a molecular beam in the presence of an electric field. The general trend of the polarizability with cluster size indicates that sodium clusters are behaving like small chunks of metal, but there is a fine structure in the experimental polarizability which cannot be explained with simple models that neglect the true geometry of the cluster. Recent measurements of the total photoabsorption cross section of alkali-metal clusters[2-4] have been fitted to a collective resonance model,[5] which uses the principal values of the static polarizability tensor as fit parameters. These experiments provide therefore information on the anisotropy of the polarizability tensor which depends on the shape of the cluster.

Presently, direct structural data for alkali-metal clusters is limited to the electron-spin-resonance results for trimers and heptamers in a rare gas matrix.[6,7] Indirect evidence on the structure of clusters can be obtained by comparing properties calculated for different isomers with the experimental values. In this paper we show that structural information on the geometry of very small sodium clusters can be obtained by comparing our calculations of the static electric dipole polarizability with the measurements of the average polarizability and of the absorption cross section. The good agreement between theory and experiment that we obtain suggests that the equilibrium geometries predicted by first-principles calculations are reliable.

Electrons in small alkali-metal clusters have delocalized wave functions and lack directionality in the bonding charge because of the weak scattering of the ionic cores.[8] If we assume that the details of the ionic scattering can be neglected and that the main role of the ions is to provide an attractive confining potential for the electron motion, then the electronic structure should manifest shell effects for the same reason that a shell structure is observed for the nucleons confined in the atomic nuclei. An important consequence of the shell model is that clusters with closed electronic shells should have an almost spherical valence-electron cloud and higher relative stabilities. The "magic numbers" of higher relative cluster abundance observed in the mass spectra of carefully prepared molecular beams of alkali-metal clusters[9] indicate that their shell structure is the same as the one obtained in a spherical jellium model of the alkali-metal

clusters.[10,11] The success of spherical jellium models in predicting the shell structure confirms that neglecting the position of the ionic cores is a reasonable first approximation. For open-shell clusters the valence-electron cloud deviates from the spherical shape, the distribution of the ions follows the electronic distribution to minimize the energy, and the geometric shape of the clusters deviates from the most compact forms.[8,12] These deviations from sphericity explain why the spherical jellium models fail to predict the detailed behavior of ionization potentials[10] or static polarizabilities (see Fig. 1), despite the fact that shell effects are observed in both experiments.[1,13] Deviations from compact structures are more important for the very small clusters because the relative number of electrons in open shells is larger, in particular the *ab initio* calculations predict that alkali-metal clusters with six atoms or fewer have planar or flattened structures.[8,14]

The static electric dipole polarizability (in the remainder of this paper we will designate this quantity simply by polarizability) α is a symmetric tensor of rank two with principal elements α_i, and we will use the indexes $i=1,2,3$ or $i=xx,yy,zz$ depending on the convenience of either notation. The average polarizability

$$\bar{\alpha}=\tfrac{1}{3}\sum_{i=1}^{3}\alpha_i \tag{1}$$

is one-third of the trace of the polarizability tensor. The *classic* static polarizability of a conducting sphere of radius R is $\alpha=4\pi\epsilon_0 R^3$ or, in atomic units (a.u.) ($\hbar=m=e=4\pi\epsilon_0=1$) which will be used in this paper, $\alpha=R^3$. The classical polarizability of a sphere with an isotropic dielectric constant ϵ and radius R is $\alpha=R^3(\epsilon-1)/(\epsilon+2)$.[15] The polarizability of a conducting ellipsoid along the principal axes i is given by[15]

$$\alpha_i=\frac{V}{4\pi n_i}\ , \tag{2}$$

where V is the volume of the ellipsoid and $n_i\geq 0$ are the depolarization factors. The dependence of n_i on the ratios of the three principal axes of the ellipsoid can be given in a closed form,[15] with larger values of $1/n_i$ corresponding to the longer ellipsoidal axis. Using the sum rule for the depolarization factors,[15]

$$\sum_{i=1}^{3} n_i=1\ , \tag{3}$$

it is easy to prove that among all ellipsoids with the same volume the minimum average polarizability $\bar{\alpha}$ is obtained for the sphere which has the depolarization factors $n_i=\frac{1}{3}$. For a perfect conductor with an arbitrary shape, the principal elements are still proportional to the volume V, but the depolarization factors must be found numerically. These expressions for the macroscopic (classical) electrostatic polarizability gives us the most important properties of the polarizability, namely (i) it is proportional to the volume and therefore to the number of atoms in the cluster, (ii) it is shape sensitive, and (iii) it depends on the electronic structure.

The simplest model for the polarizability of an alkali-metal cluster with n atoms assumes that it behaves like a perfect conducting sphere with radius $R=R_0$, where $R_0^3=3n/4\pi\rho_{\rm at}$, and $\rho_{\rm at}$ is the atomic density of the bulk metal. For sodium clusters, this model predicts that $\alpha=4\pi\epsilon_0 n\times 9.4$ Å^3, that is, the polarizability per atom is 40% of the atomic value, a correct ballpark figure. A better model can be obtained if we take into account that the electronic charge density has a tail into the vacuum region, which is very effective in screening electric fields. It has been found in model jellium calculations of surfaces that the center of gravity of the image charge is at a distance t from the jellium edge. Including the effect of this "spill out" of the electronic charge leads to the prediction[16] that the cluster polarizability should be $\alpha=(R_0+t)^3$. The curve using the jellium value for Na of Ref. 16, $t=0.5$ Å, is compared in Fig. 1 with the experimental results. We can see that this simple model already accounts for the slow decrease of the normalized cluster polarizability α/n from the atomic to the bulk value.

The experimental average polarizability of Na_n clusters (Fig. 1) shows a distinct minimum for the closed-shell Na_2 and Na_8 clusters, and it drops again when the region of the next closed-shell clusters Na_{18} and Na_{20} is reached. This can be explained with classical electrostatics if the clusters are modeled as ellipsoidal perfect conductors, and if it is assumed that the closed-shell clusters are spherical, while open-shell clusters deviate from the spherical shape.[12] Indeed the classical conducting ellipsoid model predicts that compact geometries corresponding to closed electronic shells have smaller polarizabilities than less compact geometries. In the particular case of a spheroidal shape the average polarizability increases by a factor of $1+2e^4/25$, where e is the eccentricity of the spheroid, with respect to the spherical shape.[15] This re-

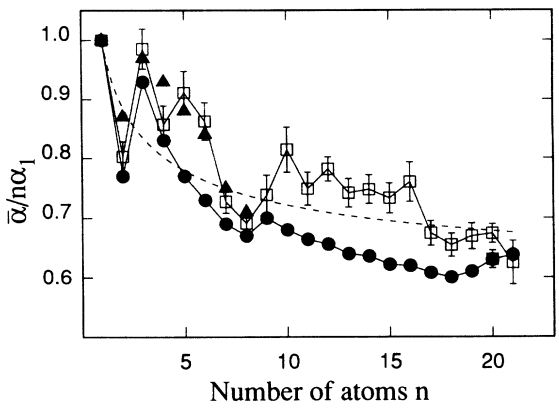

FIG. 1. Comparison of previous results of the polarizability divided by n times the atomic values with the experimental results (squares) of Knight *et al.* (Ref. 1). The solid circles correspond to jellium calculations of Manninen *et al.* (Ref. 17) and the solid triangles are the model potential results of Manninen (Ref. 24). The dashed line shows the results from the "spill out" model $\alpha=(R+t)^3$. Notice that the fine structure of the experimental polarizability between two closed shells is not reproduced by these calculations.

lationship between the polarizability and cluster shape has been used by Clemenger[12] to explain the relative minima of the polarizability observed for the closed-shell clusters with $n=2$, 8, and 18 (Fig. 1).

The response of metal clusters to static electric field has been the subject of several theoretical investigations.[16–24] Most of these calculations[16–20] have been performed assuming a spherical potential for the electron-ion interaction (spherical jellium model) and have used self-consistent linear response theory to calculate the polarizability. The spherical jellium polarizabilities calculated for sodium[17] are shown in Fig. 1, and are only marginally better than the predictions of the much simpler "spill out" model. Although they present minima at shell closings as the experiments, they do not describe the fine structure of the polarizability between two closed shells, and they predict polarizability magnitudes that are between 10% and 30% lower than experiment. The underestimation of the magnitude of the polarizability is in part an effect of the local-density approximation used in the calculations,[25] while the failure to describe the fine structure is due to the oversimplification of the spherical approximation.

Good agreement with experiment has been obtained in calculations of the polarizability of alkali-metal dimers[21–23] and trimers[23] using quantum-mechanical calculations and their real geometry. Manninen[24] calculated the polarizability of sodium clusters with up to eight atoms using realistic geometries but an approximate expression for the total energy. These calculations predict a strong anisotropy of the polarizability tensor, but the calculated average cluster polarizability does not reproduce the observed fine structure of the polarizability, in particular for the case of Na_4 (see Fig. 1).

We present in this paper realistic pseudopotential local-spin-density (LSD) calculations of the electric properties of sodium molecules up to nine atoms. The equilibrium geometries are determined from the minimization of the calculated total energy, and the polarizability is calculated from the response of the clusters to a finite static electric field. We find that the electric field is well screened inside a cluster and that the ionic contribution to the polarizability can be neglected. We find that the polarizability tensor can be strongly anisotropic, and that this anisotropy is related to both the electronic and geometric structure of the clusters. We also estimated the effects of the molecular vibrations on the polarizability for dimers and trimers[23] and found that they are not large.

Our calculations of the static polarizability of Na_n clusters ($1 \le n \le 9$) are in good agreement with the experimental trend. This confirms that the cluster geometrical structure is indeed responsible for the fine structure of the polarizabilities and suggests that the geometric structures predicted by *ab initio* calculations are essentially correct.

II. THEORY

Our calculations are performed in the local-spin-density approximation of the density-functional formalism.[26] The electronic structure of the clusters is obtained from the self-consistent Kohn-Sham single-particle equations

$$[-\tfrac{1}{2}\nabla^2+u(\mathbf{r})+v_{\rm xc}(\mathbf{r})+v_{\rm ext}(\mathbf{r})]\psi_{j\sigma}(\mathbf{r})=\varepsilon_{j\sigma}\psi_{j\sigma}(\mathbf{r}) , \quad (4)$$

where $\psi_{j\sigma}$ is the jth one-electron wave function with spin σ and eigenvalue $\varepsilon_{j\sigma}$, and

$$u(\mathbf{r})=\int \frac{\rho(\mathbf{r}')}{|\mathbf{r}-\mathbf{r}'|}d^3r' \quad (5)$$

is the Hartree potential. The electron density is

$$\rho(\mathbf{r})=\sum_j f_{j\sigma}|\psi_{j\sigma}(\mathbf{r})|^2 , \quad (6)$$

where the occupation numbers $f_{j\sigma}$ of the spin orbitals ($0 \le f_{j\sigma} \le 1$) are given by the building-up ("*Aufbau*") principle. For the exchange correlation potential $v_{\rm xc}(\mathbf{r})$, we use the Ceperley and Alder values for an homogeneous electron gas[27] as parametrized by Perdew and Zunger.[28] The external potential

$$v_{\rm ext}(\mathbf{r})=v_{e\text{-ion}}(\mathbf{r})+\mathbf{F}\cdot\mathbf{r} \quad (7)$$

includes the electron-ion potential and, when we calculate the polarizability, it also includes the interaction with an applied static inhomogeneous electric field $\mathbf{F}$. We use two different nonlocal pseudopotentials for the electron-ion interaction; the first is an *ab initio* local-density norm-conserving pseudopotential parametrized by Bachelet, Hamman, and Schlüter (BHS),[29] the second is an empirical nonlocal pseudopotential fitted by Bardsley[30] to the excitation spectrum of atomic sodium.

The details of the computational method were described previously[8] and we will restrict ourselves to a brief description. The molecular orbitals for the valence wave functions are expanded in a Gaussian basis set ($3s3p$) whose exponents are shown in Table I. The main difference with respect to the basis set used by some of us in previous calculations[8] is that we add a more extended p Gaussian to improve the convergence of the calculated polarizability. Calculations with larger basis sets show that the molecular properties are well converged with respect to the basis-set size. We use auxiliary Gaussian basis sets[31] to fit the Hartree and exchange-correlation potentials. In the auxiliary basis sets we include Gaussians with l-1 angular momentum centered on the molecular center to improve the fit of the polarization charge. From our convergence tests, we estimate that the error in the polarizabilities due to the auxiliary basis set incompleteness is less than 1%.

The equilibrium structure of the clusters is found by minimizing its total energy,

$$E_{\rm tot}=E_{\rm kin}+E_H+E_{\rm xc}+E_{e\text{-ion}}+E_{\rm ion\text{-}ion}+E_{\rm int} , \quad (8)$$

which is the sum of the kinetic, Hartree, local-density exchange and correlation, electron-ion, ion-ion, and interaction with electric-field contributions. The last term is given explicitly by

$$E_{\rm int}=\int \rho(\mathbf{r})\mathbf{F}\cdot\mathbf{r}\,d^3r . \quad (9)$$

TABLE I. Exponents of the Gaussian basis functions.

3s	3p
0.030 466	0.025 091
0.086 586	0.088 611
0.397 668	0.640 266

We use the calculated Hellmann-Feynman forces in our search for the energy minima.[32]

The dipole moment μ for a neutral cluster is the sum of the ionic and electronic contributions,

$$\mu=\mu^{\text{ion}}+\mu^{\text{el}}=\sum_j Z_j\mathbf{R}_j-\int \mathbf{r}\rho(\mathbf{r})d^3r\ , \tag{10}$$

with Z_j and $\mathbf{R}_j$ being respectively the charge and the position of the jth core, and $\rho(\mathbf{r})$ is the electron density. Note that low-symmetry molecules may have permanent dipole moments μ_0 in the absence of applied external fields.

The symmetric polarizability tensor α is the derivative of the induced dipole with respect to the electric field $\mathbf{F}$,

$$\mathbf{p}_{\text{ind}}(\mathbf{F})=\mu(\mathbf{F})-\mu_0=\alpha\cdot\mathbf{F}+O(\mathbf{F}^2)\ . \tag{11}$$

This derivative is calculated numerically from the solutions of the Kohn-Sham equations in the presence of the static electric potential $\mathbf{F}\cdot\mathbf{r}$.

For all our calculated ground-state geometries, the principal axes of the symmetric polarizability tensor are uniquely determined by the symmetry of the cluster, and therefore the principal elements of the polarizability tensor are obtained from the induced polarization charge of the molecule for a few values of the electric field oriented along each of the principal axes of the molecule. The electric-field values we use are in the range from 5×10^7 to 25×10^8 V m^{-1} (10^{-4} to 5×10^{-3} a.u.) compared to the atomic ionization field of about 2×10^{10} V m^{-1}. For those values of $\mathbf{F}$, we avoid numerical noise in the calculation of the numerical derivatives and we are still within the linear-response regime.

If the ionic positions are not allowed to relax (which is a good approximation for Na clusters), the static polarizability can also be calculated from the energy difference

$$\begin{aligned}\Delta E&=E_{\text{tot}}(\mathbf{F})-E_{\text{tot}}(0)\\&=-\mu_0\cdot\mathbf{F}-\tfrac{1}{2}\mathbf{F}\cdot\alpha\cdot\mathbf{F}+O(\mathbf{F}^3)\ .\end{aligned} \tag{12}$$

This therefore provides a check on the consistency of our calculations. We note that because of the self-consistent nature of the calculations, this energy difference is not the interaction term E_{int} of Eq. (9) which corresponds to the energy of a static dipole in an external field. Indeed, the energy used to create the induced dipole moment has contributions from the kinetic, Hartree, exchange-correlation, and electron-ion terms.

III. RESULTS AND DISCUSSION

A. Equilibrium properties

In Fig. 2(a) we show the calculated ground-state equilibrium geometries of sodium aggregates with nine atoms or fewer, and in Fig. 2(b) the geometry of the interesting

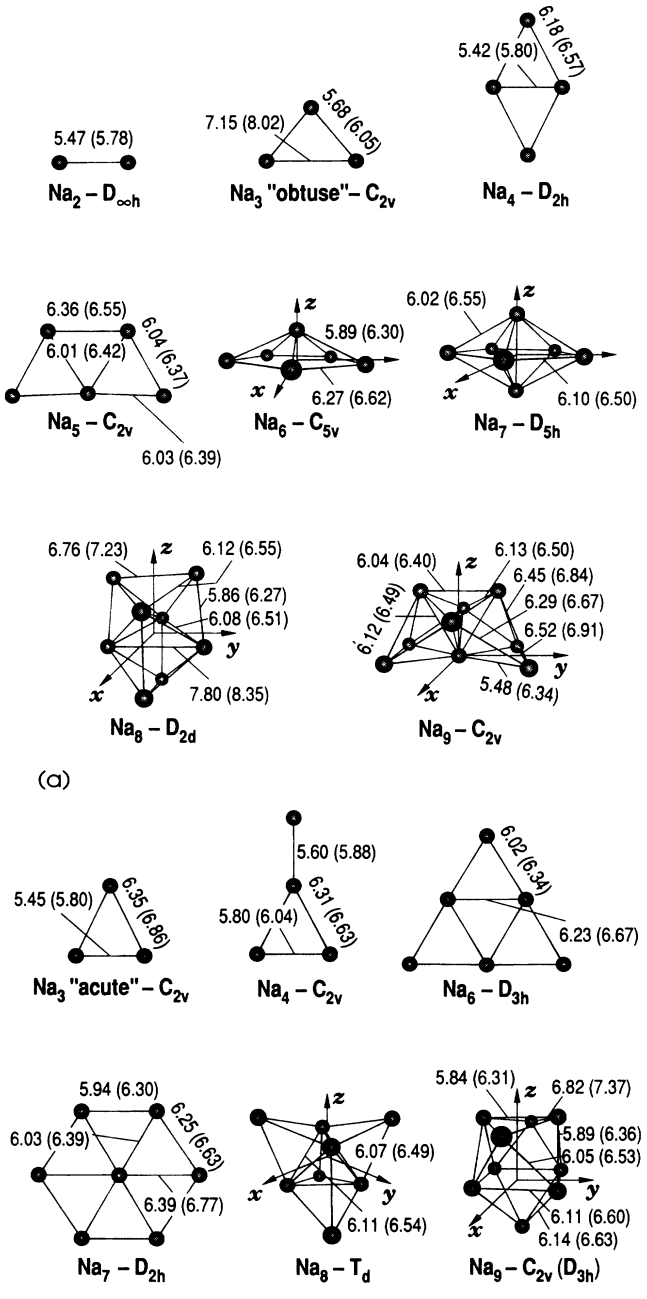

FIG. 2. Calculated equilibrium geometries (a) and lowest-lying geometries (b) of Na_n with $n\leq9$. The interatomic distances calculated with the *ab initio* BHS pseudopotential are shown and we report in parenthesis those calculated with the empirical Bardsley pseudopotential. For the planar geometries the atoms are in the xy plane, the x axis being horizontal, and for the 3D clusters the coordinate axis is drawn for each cluster.

low-energy isomers of Na_n for $n=3$, 4, 6, 7, 8, and 9. The results are practically identical to those of Martins *et al.*,[8] which is not surprising, since the two calculations differ only in minor numerical details such as the choice of basis sets. They also agree in general with the geometries obtained in extensive configuration-interaction (CI) calculations for sodium[14] and in other *ab initio* calculations for small alkali-metal clusters.[33,34] The relationship of these geometries to the underlying electronic structure has been discussed previously.[8] Modern *ab initio* calculations are quite reliable in their predictions of relative molecular energies, but when two isomers have differences in energy which are smaller than the typical errors of the local-density approximation or to the finite size of the configuration-interaction expansion, then it is not possible to predict with confidence which of the isomers corresponds to the ground state. Our discussion of the geometries of sodium clusters will therefore focus on the case where there are low-energy isomers.

The calculated energy differences between the ground states and their isomers are presented in Table II for the interesting cases. For Na_3, all recent *ab initio* calculations predict that the equilibrium geometry is an "obtuse" isosceles triangle, (here "obtuse" and "acute" are used to label an isosceles triangle with an apex angle larger or smaller than 60°). They also agree that the Born-Oppenheimer surface has a saddle point for an "acute" isosceles triangle which is only a few tens of a meV above the ground state. The Born-Oppenheimer surface of Na_3 has been discussed previously,[31] and the electron-spin-resonance spectrum of Na_3 in a rare-gas matrix is consistent with an "obtuse" ground-state geometry[6] and the existence of a low-lying saddle point. For Na_4 and Na_7 the difference in energy is sufficiently large that we are confident that the equilibrium geometries are the diamond and pentagonal bipyramid. Moreover, for Na_7, the three-dimensional pentagonal-bipyramid ground state is in agreement with electron-spin-resonance experiment.[7] The T-shaped isomer of Na_4 and the planar isomer of Na_7 obtained from a Jahn-Teller distortion of a symmetric centered hexagon [see Fig. 2(b)] are included in our calculations only to test if the experimental polarizability can be used to identify the stable isomer.

For Na_6, Na_8, and Na_9 the difference in energy between the isomers (Table II) is of the order of one or two percent of the binding energy of the cluster, and theoretical calculations cannot predict with confidence which geometry is the true ground state. The calculated energy difference between the local minimum of the Na_6 Born-Oppenheimer surface with a planar geometry (D_{3h} point-group symmetry) and the pentagonal pyramid ground-state geometry is 124 meV, whereas in previous local-density calculations[8] that difference was 40 meV. In both calculations, the energy difference is in favor of the three-dimensional geometry, while CI calculations predict the planar geometry to be more stable (see Table II). Within the expected accuracy of local-density calculations, the two geometries have the same energy and the actual ground state of Na_6 could be either one of the isomers. The calculated equilibrium geometry For Na_8 has the D_{2d} point-group symmetry as found previously in local-density calculations.[8] The tetrahedral geometry proposed by Bonačić-Koutecký *et al.*[14] is found to be an isomer with total energy 67 meV higher. The energy difference of 8 meV per atom is very small and the true ground state cannot be distinguished within the precision of our calculations. We note that the interatomic distances for Na_8 were incorrectly reported in Ref. 8; the correct bond-length values from that work are in agreement with the present calculations.[35] For Na_9, we find two isomers very close in energy (see Table II). The ground-state geometry is very similar to that proposed by Bonačić-Koutecký *et al.*[14] but has a higher symmetry (C_{2v} point group instead of C_s). The lowest-lying isomer of Na_9 also has the C_{2v} symmetry and is obtained from a Jahn-Teller distortion of the more symmetric D_{3h} geometry with a Jahn-Teller stabilization energy of 11 meV [see Fig. 2(b)]. This isomer is labeled as C_{2v} (D_{3h}) in this paper.

The Bardsley empirical pseudopotential leads to the same symmetry as the *ab initio* BHS pseudopotential for the equilibrium ground states of clusters with up to eight atoms. However, the interatomic distances are consistently 7% larger (Fig. 2), improving the agreement with the experimental bond length for Na_2, and presumably also for the other clusters. The energy difference between the ground state and the lowest isomer reported in Table II is fairly insensitive to the choice of pseudopotential, except for Na_9 where it has the opposite sign, indicating that the C_{2v} (D_{3h}) geometry has the lowest energy when we use the empirical pseudopotential, and illustrating the limitations of total-energy calculations in the presence of isomers that are very close in energy. The calculated absolute values of the dissociation energies of the ground states of Na_n (Table III) are smaller for the empirical pseudopotential, improving again the agreement with available experimental data, but the dissociation channels are still the same. The dissociation energies for Na_2 and Na_3 overestimate the experimental values, as has been observed in other molecular local-density calculations.[36,37]

The existence of a permanent dipole moment for Na_n is dictated by the symmetry of the molecules. The clusters with a permanent dipole moment, namely both geometries of Na_3, the T shape of Na_4, Na_5, the three-

TABLE II. Energy difference ΔE in meV between the ground state and the lowest-lying isomer of Na_n (see Fig. 2). We show our values calculated with the *ab initio* pseudopotential (BHS) and the empirical Bardsley pseudopotential (Brd). We also present in the last column the results from pseudopotential CI calculations (Ref. 14).

	ΔE (BHS)	ΔE (Brd)	ΔE (CI)
Na_3	29	28	
Na_4	249	188	136
Na_6	124	90	−46
Na_7	813	690	
Na_8	67	107	
Na_9	41	−174	

TABLE III. Dissociation energies of Na_n in eV calculated with the BHS *ab initio* pseudopotential and the Bardsley empirical pseudopotential (Brd). The underlined values indicate the preferred dissociation channel. We report in the last row the experimental dissociation energy.

n	2	3	4	5	6	7	8	9
BHS								
Na, Na_{n-1}	0.89	0.48	1.05	0.83	1.22	1.33	1.17	0.71
Na_2, Na_{n-2}			0.63	0.99	1.16	1.67	1.61	0.99
Na_3, Na_{n-3}					1.73	2.01	2.35	1.84
Na_4, Na_{n-4}							2.13	2.02
Experiment	0.75[a]	0.33[b]						
Bardsley								
Na, Na_{n-1}	0.83	0.40	0.95	0.78	1.13	1.14	1.14	0.66
Na_2, Na_{n-2}			0.52	0.90	1.09	1.45	1.45	0.93
Na_3, Na_{n-3}					1.64	1.83	2.18	1.68
Na_4, Na_{n-4}							2.01	1.86
Experiment	0.75[a]	0.33[b]						

[a]Reference 39.
[b]Reference 42.

dimensional geometry of Na_6, and both geometries of Na_9 have the C_{nv} symmetry with μ_0 parallel to the n-fold axis. The values of μ_0 calculated using the *ab initio* BHS pseudopotential and the empirical Bardsley (Brd) pseudopotential are reported in Table IV. For the ground state of Na_3, Na_5 and the C_{2v} geometry of Na_9, the very small values of the permanent dipole moment reported in Table IV and the change of sign observed with different pseudopotentials indicate that μ_0 is negligible for these molecules. These small values result, however, from the cancellation of rather large contributions of the individual orbitals. In particular, for the "obtuse" trimer, the individual contribution to μ_0 of the bonding and the nonbonding orbitals are respectively equal to -0.367 and 0.365 a.u., the positive and negative sign can easily be traced back to the charge transfer expected for these orbitals from elementary molecular-orbital theory. The permanent dipole moment is therefore very sensitive to the geometry of the clusters, and different cluster geometries can have very different values of μ_0. The T shape of the tetramer presents a large permanent dipole moment, whereas the ground-state geometrical structure has by symmetry a zero dipole moment, the dipole of the planar geometry of Na_6 (D_{3h} symmetry) is zero, while the pentagonal pyramid has a permanent dipole moment of about -0.5 a.u. oriented along the fivefold axis. The permanent dipole is a quantity which is very delicate to calculate, and we see from Table IV that the two pseudopotentials give values for the permanent dipole that can differ by 0.09 a.u. or less.

TABLE IV. Permanent dipole moment $\mu^{el}=\mu$ of Na_n in a.u. We show the values calculated with the *ab initio* BHS pseudopotential (BHS) and the empirical Bardsley pseudopotential (Brd).

	BHS	Brd
Na_3 ("obtuse")	-0.002	0.005
Na_3 ("acute")	-0.256	-0.318
Na_4 (T shape)	-1.123	-1.171
Na_5	0.010	-0.014
Na_6 (C_{5v})	-0.511	-0.453
Na_9 (C_{2v})	0.028	-0.013
Na_9 [C_{2v} (D_{3h})]	0.132	0.046

B. Static polarizabilities

For the small clusters with $n \leq 4$, we have optimized the geometry in the presence of the perturbation and have found that the contribution of the ionic relaxation to the induced dipole moment [see Eq. (10)] is $\approx 1\%$ of the total induced dipole. This shows that the external electric field at the nuclear sites can be assumed to be completely screened. The dependence of the induced dipole moment of Na_5 on the strength of the applied electric field is shown in Fig. 3 for three different directions.

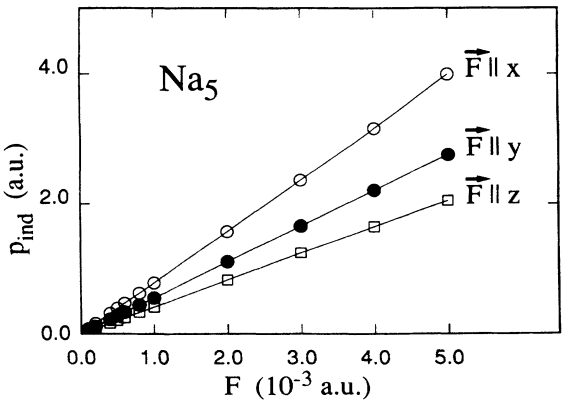

FIG. 3. Induced dipole moments vs the electric field for Na_5. The electric field is oriented along each of the principal axes of the molecule.

These directions are by symmetry the principal directions of the polarizability tensor, therefore the slope of the lines give the three principal elements of the polarizability. The figure also shows that for the electric-field values used in our calculations the response is linear.

The principal values of the polarizability tensor calculated with the *ab initio* BHS pseudopotential for each cluster size are shown in Table V. The tensor shows a strong anisotropy (see also Fig. 3), which reflects the deviation of the geometry of the molecule from compact shapes and is closely related to the extension of the electron density along the principal axes of the molecule. This is illustrated for Na_5 in Fig. 4, where we present the pseudopotential valence electron density in the plane containing the five atoms [Fig. 4(a)] and in a plane perpendicular to the C_2 point-group symmetry axis [Fig. 4(b)]. The decreasing extension of the charge densities along the x, y, and z directions is correlated with a decrease in the polarizability $\alpha_{xx} > \alpha_{yy} > \alpha_{zz}$ (Table V). For the Na_8 isomer with the tetrahedral symmetry, all three diagonal elements of the tensor are identical by symmetry, while for both isomers of Na_6, the 3D isomer of Na_7 and the D_{2d} octamer the polarizability in the x and y directions is identical by symmetry. In our calculations the numerical fit of the exchange and correlation potential breaks the symmetry of the cluster and the calculated values for degenerate polarizabilities differ by less than 1%, which is within our estimations of the numerical noise associated with the fitting procedure.

Another way of understanding qualitatively the anisotropy of the polarizability tensor is to use perturbation theory to calculate the second-order correction to the energy within the independent-electron model,

$$\Delta E_{\mathrm{IEM}} = \sum_{i,\sigma'} \sum_{j,\sigma} f_{i\sigma'}(1-f_{j\sigma})\delta_{\sigma\sigma'} \frac{|\langle \psi_{i\sigma'}|\mathbf{F}\cdot\mathbf{r}|\psi_{j\sigma}\rangle|^2}{\epsilon_{i\sigma'}-\epsilon_{j\sigma}} . \tag{13}$$

Although this expression neglects screening, the magnitude of the correction gives qualitatively the change in total energy ΔE in the presence of the electric field and therefore, through Eq. (12) the values of the polarizability tensor elements. Selection rules for the coupling of the one-electron Kohn-Sham orbitals for each direction of the electric field give an indication of the order of magnitude of the polarizability tensor elements. For Na_2, for example, the occupied valence bonding orbital is coupled to the lowest empty state, the Σ antibonding orbital, when the electric field is parallel to the axis of the molecule, but is coupled to a higher, empty Π orbital when the electric field is perpendicular to the molecular axis. As the energy difference appears in the denominator of Eq. (13), the perpendicular component of the polarizability tensor will therefore be smaller than the parallel element. For the planar geometries ($n \leq 5$), we find that when the field lies in the molecular plane, the occupied molecular orbitals are coupled with nearby empty orbitals, both coupled orbitals being linear combinations of atomic s orbitals. For electric fields perpendicular to the molecular plane, there is a coupling with orbitals that are linear combinations of atomic p orbitals which are higher in en-

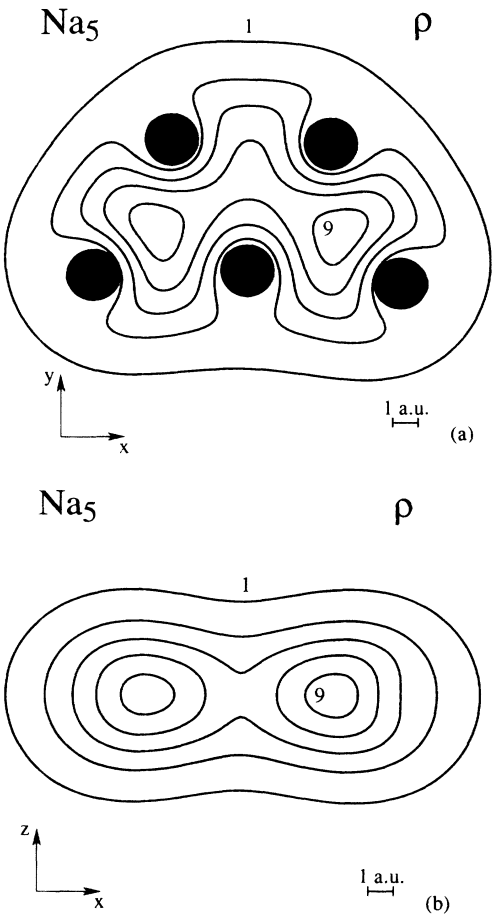

FIG. 4. Electron density of Na_5 in the plane of the molecule (a) and in a plane perpendicular to the atoms (b). The contours lines of equal density are spaced by 2×10^{-3} a.u. The solid regions indicate the extent of the atomic cores.

TABLE V. Principal values in Å^3 of the polarizability tensor of Na_n clusters calculated with the *ab initio* BHS pseudopotential.

	α_{xx}	α_{yy}	α_{zz}
Na	21.0	21.0	21.0
Na_2 ($D_{\infty h}$)	47.2	26.1	26.1
Na_3 (C_{2v} "obtuse")	78.8	46.6	36.0
Na_3 (C_{2v} "acute")	50.6	74.3	34.2
Na_4 (D_{2h})	49.9	104.8	46.6
Na_4 (C_{2v} T shape)	75.6	123.2	57.4
Na_5 (C_{2v})	118.3	81.9	60.9
Na_6 (D_{3h})	117.4	115.1	67.5
Na_6 (C_{5v})	105.1	105.2	57.9
Na_7 (D_{5h})	99.7	100.1	75.4
Na_7 (D_{2h})	144.5	129.8	71.1
Na_8 (D_{2d})	93.2	92.6	105.3
Na_8 (T_d)	105.6	105.3	105.0
Na_9 (C_{2v})	96.8	105.6	136.4
Na_9 [C_{2v} (D_{3h})]	94.8	107.3	150.4

ergy, so that the polarizability is smaller for that direction.

The measured polarizabilities[1] were interpreted as being the average of the polarizability over all the orientations of the molecule because of the molecular rotational motion. This assumes that in the conditions of that experiment the energy scale associated with the rotational temperature of the clusters is larger than the electric dipolar energy of the molecule in the external electric field. Therefore we will compare the experimental values with the calculated average polarizability $\bar{\alpha}$.

We show in Figs. 5(a) and 5(b) the rotationally averaged polarizability $\bar{\alpha}$ and the normalized polarizability $\bar{\alpha}/n\alpha_1$ of the calculated ground state of Na_n clusters obtained with the two different pseudopotentials. We also show the polarizability values calculated for the lowest-lying isomers shown in Fig. 2(b). Figure 5(b) shows that the trend of our results is in good agreement with experiment, and in particular the fine structure of the polarizability between the closed shells $n=2$ and 8 is well reproduced, including the odd-even alternation appearing for clusters up to $n=6$ and its disappearance for $n=7$ and 8. Previous calculations (see Fig. 1) predicted a structureless decrease of the normalized polarizability from $n=3$ to 8.

We have indicated by a dashed line in Figs. 5(a) and 5(b) the trend we obtain when we assume that the planar isomer of Na_6 is the one observed in the experiment. The agreement with the experimental trend is improved, in particular there is a strong increase of $\bar{\alpha}$ from Na_5 to Na_6 and a plateau between Na_6 and Na_7 [see Fig. 5(a)]. This improvement in the agreement between theory and experiment is an indication that the geometry of Na_6 may be planar. At this point we should make two comments concerning the experimental conditions. First, the experimental error bars in the polarizability are non-negligible (see Fig. 5) and they should be taken into account in the matching of the polarizability trends. Second, the temperature of the clusters in the molecular beam is finite, and therefore isomers that are very close in energy could be simultaneously present in the molecular beam.

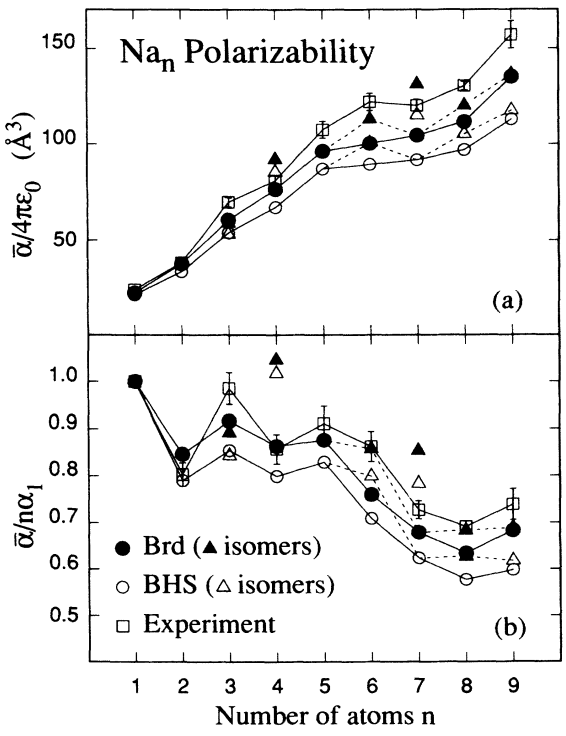

FIG. 5. Rotationally averaged polarizabilities $\bar{\alpha}$ (a) and normalized polarizabilities $\bar{\alpha}/n\alpha_1$ (b) of the Na_n clusters. The solid circles correspond to our numerical values calculated with the Brd empirical pseudopotential, the open circles are the values calculated with the *ab initio* BHS pseudopotential. The squares represent the experimental results. The open and solid triangles correspond, respectively, to the isomer geometries calculated with the BHS and Bardsley (Brd) pseudopotentials. The lines are only a guide for the eye.

The observed plateau of $\bar{\alpha}$ and the related strong decrease of the normalized polarizability from Na_6 to Na_7 is what should be expected for a transition from planar to more compact three-dimensional geometries. We also note that the normalized polarizabilities of the higher-energy isomers of Na_4 and Na_7 are in complete disagreement with the experimental results, which shows that we can use the comparison between theory and experiment to identify the equilibrium geometry. In the case of Na_7, our results confirm that the plateau in the polarizability is associated with a change of dimensionality.

Although for Na_8 the polarizability of the T_d isomer is closer to the experimental value [Fig. 5(a)], the inspection of the general trend suggests that the D_{2d} geometry may be the one observed in the deflection experiment. However, if we notice that our calculations consistently underestimate $\bar{\alpha}/n\alpha_1$ for odd n, and are very accurate for an even number of atoms, which is attributed to a spurious local-density effect, then we obtain a better agreement with experiment if we assume the T_d geometry to be the most stable. The values for the two geometries of Na_9 are very similar, so that the comparison with experiment does not allow us to distinguish the experimental ground state.

From the above discussion we can see that for clusters with up to seven sodium atoms the calculations suggest few candidates for the ground-state geometry, and these structures have significantly distinct polarizabilities. For sizes larger than eight atoms the number of configurations with similar energies increases, traditional gradient methods of energy minimization get stuck often in local minima, and different geometries have similar polarizabilities. Therefore our comparison of theoretical and experimental polarizabilities can only provide evidence for the geometry of Na_n clusters when $n<8$.

Recent measurements of the total photoabsorption cross section of alkali-metal clusters[2-4] have been fitted to a collective resonance model,[5] which uses the the principal values of the static polarizability tensor as fit parameters for the resonance frequency,

$$\omega_i^2=\frac{ne^2}{m_e\alpha_i} .$$

These experiments can be very helpful for the identification of cluster geometries because they have in-

formation on the anisotropy of the polarizability tensor. The results[3] for Na_4 indicate that there are two main resonance peaks in the photoabsorption spectra. The D_{2h} ground-state geometry of Na_4 has three distinct polarizability values (Table V), but two are quasidegenerate and therefore should appear in experiment as a single broader resonance. The C_{2v} isomer geometry of Na_4 has three distinct principal values of the polarizability, and is not consistent with the experimental observations. The photoabsorption spectra is therefore consistent with a ground-state D_{2h} geometry for Na_4. The published measurements[2,3] of the photoabsorption of Na_8 indicate that there is a single resonance peak around 490 nm. The value, calculated from our numerical polarizabilities renormalized to the experimental atomic polarizability, is 475 nm in the case of T_d geometry. For the D_{2d} geometry, we predict two resonances at 446 and 481 nm. Considering that the resonance width is about 70 nm, a line-shape analysis and a better understanding of the validity of the plasmon model may be required to reach a definitive conclusion. At this point, we can then only conclude that both the T_d and D_{2d} geometries are in agreement with experiment. Notice also that in the experimental molecular beam, both T_d and D_{2d} geometries could be present. The experimental results for Na_9 (Ref. 2) indicate that, of the three resonance peaks, two are degenerate or quasidegenerate, and the third corresponds to a polarizability that is 1.7 times larger. That would agree better with the calculated factor of 1.6 for the anisotropy of the polarizability of the capped triangular prism [C_{2v} (D_{3h})] isomer.

The absolute values of the averaged polarizability calculated with the *ab initio* BHS and the empirical Bardsley pseudopotential [see Fig. 5(a)] underestimate the experimental results, but the discrepancy is reduced from about 20% to 10% when the empirical Bardsley pseudopotential is used. We note that with the Bardsley pseudopotential the agreement for Na_2 and Na_4 is excellent. The increase of the polarizability with the empirical pseudopotential is due both to the larger interatomic distances obtained and to the larger value of the atomic polarizability which is increased by 5%. For the dimer, 50% of the increase of the parallel component of the polarizability is due to the larger bond length. We attribute the discrepancy between the calculated and measured polarizabilities to the approximations made in solving the many-body problem, namely the local-spin-density and pseudopotential approximations. The atomic polarizability calculated with the Bardsley pseudopotential is 7% lower than the experimental value. Since an "exact" one-electron calculation of the atomic polarizability where the effective potential includes only the core-valence interaction described by the same pseudopotential is in perfect agreement with the experimental value of 23.6 $Å^3$, the 7% difference is a local-spin-density effect, as we discussed previously.[25] We have tried to correct the local-density approximation by introducing a self-interaction correction,[28] and have found that the sodium dimer becomes more tightly bounded and has a smaller polarizability which worsens the agreement with experiment.[25] We notice that a previous jellium calculation, using a nonstandard *ad hoc* self-interaction correction,[19] found an increase of the polarizability in complete disagreement with our results. We also estimated the influence of the ionic vibrations on the polarizability of the dimers and trimers and found it to be small, a few % at most. We present in the Appendix a discussion of these effects.

IV. CONCLUSIONS

We calculate the static electric polarizability of sodium clusters with nine atoms or fewer in their calculated ground-state equilibrium geometries and in the geometries of particularly stable isomers. We then compare the experimental trend of the average polarizability with the values calculated for different geometries and determine which geometry gives a better agreement with experiment.

For clusters sizes from Na to Na_5 and Na_7, theoretical calculations predict that there is a single serious candidate for the ground-state geometrical configuration. In these cases there is a good agreement between theoretical and experimental polarizability trends. For Na_6, Na_8, and Na_9, there are isomers with energies so close to the ground-state energy that they are possible candidates for the true ground-state configuration, when we consider the accuracy of total-energy calculations. For Na_6 a better agreement with the experimental trend is obtained for the planar isomer D_{3h} geometry than with the pentagonal pyramid C_{5v} geometry, indicating that the former strongly contributes to the measured polarizability. For Na_8 and Na_9 it is not clear which of the isomers gives better agreement with the experimental average polarizabilities.

Our work shows that the comparison of calculated average polarizabilities of cluster isomers with experiment can be used to extract structural information about which isomers are observed in experiment. The recent photoabsorption cross-section experiments contain information on the anisotropy of the electrical polarizability, and we expect that in the future calculated values of the static electrical polarizabilities for different isomers will be very important for the identification of cluster structures.

ACKNOWLEDGMENTS

The work reported in this paper was partially supported by the Fonds National Suisse de la Recherche Scientifique (Grant No. 2.859-0.88).

APPENDIX: VIBRATIONAL EFFECTS

The results presented in the main section of this paper use the clamped-nuclei approximation, that is, they assume that the nuclei do not move, or more correctly that their mass is infinite. In this Appendix we estimate the vibrational corrections to the molecular polarizability[38] of dimers and trimers in the harmonic approximation. The use of harmonic vibrational wave functions is a good approximation for Na_2 but not for Na_3, therefore we expect our estimations of the vibrational contributions for

Na_2 to be reliable, but the results for Na_3 are expected to be estimations of the magnitude.

The Schrödinger equation for the ionic vibration wave function $\chi(\mathbf{Q},\mathbf{F})$ in the presence of an external electric field and in the adiabatic approximation is

$$H_N\chi(\mathbf{Q},\mathbf{F})=[T_N+U_e(\mathbf{Q},\mathbf{F})]\chi(\mathbf{Q},\mathbf{F})=E(\mathbf{F})\chi(\mathbf{Q},\mathbf{F}) , \tag{A1}$$

where Q represents the coordinates of the nuclei, and T_N is the corresponding nuclear kinetic energy. The dependence of the adiabatic potential on the external electric field,

$$\begin{aligned} U_e(\mathbf{Q},\mathbf{F}) &= U_e(\mathbf{Q},0)-\boldsymbol{\mu}(\mathbf{Q})\cdot\mathbf{F}-\tfrac{1}{2}\cdot\mathbf{F}\cdot\alpha(\mathbf{Q})\cdot\mathbf{F}+O(\mathbf{F}^3) \\ &= U_e(\mathbf{Q},0)+\delta U_e(\mathbf{Q},\mathbf{F}) , \end{aligned} \tag{A2}$$

will be treated in perturbation theory for the calculation of the molecular polarizability. The unperturbed Hamiltonian is independent of the electric field and therefore does not contribute to the molecular polarizability. The simplest way to determine the molecular polarizability is to expand $U_e(Q,\mathbf{F})$ in powers of the normal coordinates of the molecule and to use the harmonic approximation to calculate the first- and second-order perturbation corrections. The correction to the polarizability will be obtained by collecting all the terms that are quadratic in the electric field. A quick inspection of the expression for δU_e shows that there are only two contributions that are quadratic in the electric field. The first contribution is due to the first-order perturbation of the term that is quadratic in the field, $\mathbf{F}\cdot\alpha(\mathbf{Q})\cdot\mathbf{F}$, and the second contribution is from the term that is linear in the electric field, $\boldsymbol{\mu}(\mathbf{Q})\cdot\mathbf{F}$, treated in second-order perturbation. The first-order term can be interpreted as the average of the clamped nucleus polarizability over the ground state vibrational wave functions in the harmonic approximation, and is given by[38]

$$\alpha^0+\alpha^{\mathrm{I}}=\alpha(\mathbf{Q}^0)+\tfrac{1}{4}\sum_k \frac{1}{M\omega_k}\frac{\partial^2\alpha}{\partial Q_k^2}(\mathbf{Q}^0)+O(1/M) , \tag{A3}$$

where M is the mass, ω_k is the frequency of the kth normal mode, $\mathbf{Q}^0$ are the equilibrium coordinates, and $\alpha^0=\alpha(\mathbf{Q}^0)$ is the clamped-nucleus polarizability of the molecule. Note that the leading term correction to the clamped-nucleus polarizability is of the order of $1/M^{1/2}$, and it is expected to be small since $1/M^{1/2}\approx 0.005$ a.u. for sodium.

The second-order perturbation includes a summation over all intermediate excited vibrational states and is given by[38]

$$\alpha^{\mathrm{II}}=\sum_k \frac{1}{M\omega_k^2}\left[\frac{\partial\mu}{\partial Q_k}(\mathbf{Q}^0)\right]^2+\sum_k \frac{1}{8M^2\omega_k^3}\left[\frac{\partial^2\mu}{\partial Q_k^2}(\mathbf{Q}^0)\right]^2+\sum_k\sum_{l>k}\frac{1}{2M^2\omega_k\omega_l(\omega_k+\omega_l)}\left[\frac{\partial^2\mu}{\partial Q_k\partial Q_l}(\mathbf{Q}^0)\right]^2+O(1/M) . \tag{A4}$$

In this equation, the first term is independent of the mass, and the others are of the order of $1/M^{1/2}$. Therefore, the vibrational corrections to the polarizability should be dominated by the contribution from the square of the gradient of μ.

We have calculated with the *ab initio* BHS pseudopotential the total energy of the molecules at several points of the Born-Oppenheimer surface and fitted it around the equilibrium position with a polynomial expansion. The quadratic terms yield the force matrix and the vibrational frequencies and eigenmodes are obtained by diagonalizing that matrix. The permanent dipole moment and the polarizability have also been calculated for several ionic configurations and fitted to polynomials in order to evaluate the appropriate first and second derivatives.

For the vibrational frequency of the dimer, we reproduce the results of Martins *et al.*;[8] $\omega_e=173$ cm^{-1}, the experimental value is 159.1 cm^{-1}.[39] We show in Table VI the vibrational frequencies of Na_3 calculated in the harmonic approximation from a polynomial fit of the Born-Oppenheimer surface, the unpublished values of Martins *et al.* calculated with a quadratic fit, the values obtained by Thompson *et al.*[40] using the Martins *et al.* data but including the anharmonicity and diabatic effects, and finally the experimental values.[41] We see that inclusion of anharmonicity and diabatic effects is required to obtain a good agreement with experiment.

As the normal mode of the dimer is symmetric, the dipole moment of Na_2 is always null and $\alpha^{\mathrm{II}}=0$. The correction α^{I} is smaller than 0.1 Å^3, and can be neglected for all practical purposes. For the trimers, the vibrational corrections to the polarizability are shown in detail in Table VII for each principal direction and normal mode. For α^{II}, we report only the first term of Eq. (A4), the oth-

TABLE VI. Vibrational frequencies of the sodium trimer in cm^{-1}. ω_1 corresponds to the symmetric stretching mode, ω_2 to the asymmetric mode, and ω_3 is the frequency of the bending mode.

	This work	Martins *et al.*[a]	Thompson *et al.*[b]	Expt.[c]
ω_1	154	148	142	139
ω_2	109	68	94	87
ω_3	64	63	58	48

[a]Reference 8.
[b]Reference 40.
[c]Reference 41.

TABLE VII. Vibrational corrections to the polarizabilities of Na_3 are shown in $Å^3$. See text for details.

	α^{I}_{xx}	α^{I}_{yy}	α^{I}_{zz}	$\bar{\alpha}^{I}$	α^{II}_{xx}	α^{II}_{yy}	α^{II}_{zz}	$\bar{\alpha}^{II}$	$\bar{\alpha}^{I}+\bar{\alpha}^{II}$
ω_1	−1.8	−3.4	−0.3	−1.8	1.3	0.5	0.0	0.6	−1.2
ω_2	2.5	4.1	−14.6	−2.7	0.0	0.0	0.0	0.0	−2.7
ω_3	−0.6	5.1	4.5	3.0	0.0	2.3	0.0	0.8	3.8
Total	0.1	5.8	−10.4	−1.5	1.3	2.8	0.0	1.4	−0.1

er terms being smaller. We observe that the average of the polarizability over the ground-state vibration α^{I} tends to reinforce the anisotropy of the tensor. The polarizabilities in the molecular plane increase, while the perpendicular component decreases. The overall effect of α^{I} in the average polarizability is a 3% decrease. Due to the molecular symmetry α^{II}_{zz} vanishes, and the asymmetric mode (ω_2) does not contribute to α^{II}. The motion of the atoms in the breathing mode (ω_1) tends to increase the molecular size, in particular in the x direction, therefore the major contribution of this mode is to α_{xx}. The bending mode (ω_3) which increases the molecular size in the y direction increases α_{yy} of 5%. The effect of α^{II} in the average polarizability is an increase of 2% that practically cancels the contribution from α^{I}.

This analysis shows that the contributions to the molecular polarizability from the molecular vibrational modes are very small for Na_2 and Na_3, in particular they are smaller than the errors due to the local-spin-density approximation. As their small magnitude is determined by the ratio of the electronic to the ionic mass, we expect that these corrections are also very small for the larger clusters. Anharmonic effects, neglected in our analysis, should be even smaller, or at most of the same order of magnitude in the exceptional cases of "floppy" molecules like Na_3.

*Present address: IBM Research Division, Zürich Research Laboratory, CH-8803 Rüschlikon, Switzerland.

[1]W. D. Knight, K. Clemenger, W. A. de Heer, and W. Saunders, Phys. Rev. B **31**, 2539 (1985).
[2]K. Selby, M. Vollmer, J. Masui, V. Kresin, W. A. de Heer, and W. D. Knight, Phys. Rev. B **40**, 5417 (1989).
[3]C. R. C. Wang, S. Pollack, and M. M. Kappes, Chem. Phys. Lett. **165**, 26 (1990).
[4]C. Bréchignac, Ph. Cahuzac, F. Carlier, and J. Leygnier, Chem. Phys. Lett. **164**, 433 (1989).
[5]V. Kresin, Phys. Rev. B **39**, 3042 (1989).
[6]D. M. Lindsay, D. R. Herschbach, and A. L. Kwiram, Mol. Phys. **32**, 1199 (1976).
[7]G. A. Thompson, F. Tischler, and D. M. Lindsay, J. Chem. Phys. **78**, 5946 (1983).
[8]J. L. Martins, J. Buttet, and R. Car, Phys. Rev. B **31**, 1804 (1985).
[9]W. D. Knight, K. Clemenger, W. A. de Heer, W. Saunders, M. Y. Chou, and M. L. Cohen, Phys. Rev. Lett. **52**, 2141 (1984).
[10]J. L. Martins, R. Car, and J. Buttet, Surf. Sci. **106**, 265 (1981).
[11]W. A. de Heer, W. D. Knight, M. Y. Chou, and M. L. Cohen, in *Solid State Physics,* edited by F. Seitz and D. Turnbull (Academic, New York, 1987), Vol. 40, p. 93.
[12]K. Clemenger, Phys. Rev. B **32**, 1359 (1985).
[13]M. M. Kappes, M. Schär, U. Röthlisberger, C. Yeretzian, and E. Schumacher, Chem. Phys. Lett. **143**, 251 (1988).
[14]V. Bonacic-Koutecky, P. Fantucci, and J. Koutecky, Phys. Rev. B **37**, 4369 (1988).
[15]L. D. Landau and E. M. Lifchitz, *Electrodynamics of Continuous Media* (Pergamon, Oxford, 1984).
[16]D. R. Snider and R. S. Sorbello, Phys. Rev. B **28**, 5702 (1983).
[17]M. Manninen, R. M. Nieminen, and M. J. Puska, Phys. Rev. B **33**, 4289 (1986).
[18]M. J. Puska, R. M. Nieminen, and M. Manninen, Phys. Rev. B **31**, 3486 (1985).
[19]P. Stampfli and K. H. Bennemann, Phys. Rev. A **39**, 1007 (1989).
[20]D. E. Beck, Phys. Rev. B **30**, 6935 (1984).
[21]D. M. Bishop and C. Pouchan, J. Chem. Phys. **80**, 789 (1984).
[22]W. Müller and W. Meyer, J. Chem. Phys. **85**, 953 (1986).
[23]I. Moullet, J. L. Martins, F. Reuse, and J. Buttet, Z. Phys. D **12**, 353 (1989).
[24]M. Manninen, Phys. Rev. B **34**, 6886 (1986).
[25]I. Moullet and J. L. Martins, J. Chem. Phys. **92**, 527 (1990).
[26]W. Kohn and P. Vashishta, in *Theory of the Inhomogeneous Electron Gas,* edited by S. Lundqvist and N. H. March (Plenum, New York, 1983), p. 79.
[27]D. M. Ceperley and B. J. Alder, Phys. Rev. Lett. **45**, 566 (1980).
[28]J. P. Perdew and A. Zunger, Phys. Rev. B **23**, 5048 (1981).
[29]G. B. Bachelet, D. R. Hamann, and M. Schlüter, Phys. Rev. B **26**, 4199 (1982).
[30]J. N. Bardsley, Case Stud. At. Phys. **4**, 299 (1974).
[31]J. L. Martins, R. Car, and J. Buttet, J. Chem. Phys. **78**, 5646 (1983).
[32]J. L. Martins and R. Car, J. Chem. Phys. **80**, 1525 (1984). This reference discusses the convergence of Hellmann-Feynman forces in pseudopotential calculations.
[33]H.-O. Beckmann, J. Koutecky, and V. Bonacic-Koutecky, J. Chem. Phys. **73**, 5182 (1980).
[34]B. K. Rao and P. Jena, Phys. Rev. B **32**, 2058 (1985).
[35]The bond lengths for Na_8 published in Ref. 8 are incorrectly reported. The cluster with the incorrect bond lengths is far from equilibrium and if allowed will transform into a different structure. The other properties of Na_8 reported in Ref. 8, including ground-state symmetry, binding energies, and dissociation energies correspond to the true energy minimum and are therefore correct.
[36]R. O. Jones, in *Ab-Initio Methods in Quantum Chemistry–I,* edited by K. P. Lawley (Wiley, New York, 1987), p. 413.
[37]D. R. Salahub, in *Ab-Initio Methods in Quantum Chemistry–II,* edited by K. P. Lawley (Wiley, New York,

1987), p. 447.
[38]P. K. K. Pandey and D. P. Santry, J. Chem. Phys. **73**, 2899 (1980).
[39]K. K. Verma, J. T. Bahns, A. R. Rajaei-Rizi, W. C. Stwalley, and W. T. Zemke, J. Chem. Phys. **78**, 3599 (1983).
[40]T. C. Thompson, G. Izmirlian, S. J. Lemon, D. G. Truhlar, and C. A. Mead, J. Chem. Phys. **82**, 5597 (1985).
[41]M. Broyer, G. Delacrétaz, G. Q. Ni, R. L. Whetten, J. P. Wolf, and L. Wöste, Phys. Rev. Lett. **62**, 2100 (1989).
[42]K. Hilpert and B. Bunsenges, Phys. Chem. **88**, 260 (1984).

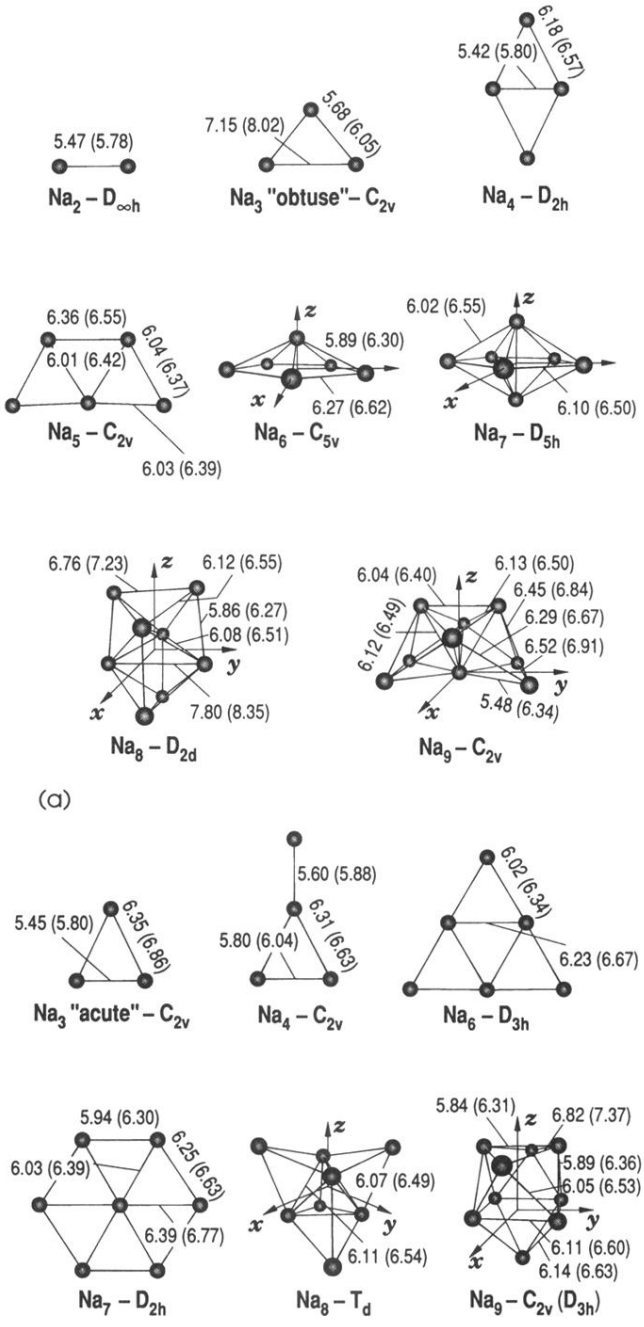

FIG. 2. Calculated equilibrium geometries (a) and lowest-lying geometries (b) of Na_n with $n \leq 9$. The interatomic distances calculated with the *ab initio* BHS pseudopotential are shown and we report in parenthesis those calculated with the empirical Bardsley pseudopotential. For the planar geometries the atoms are in the xy plane, the x axis being horizontal, and for the 3D clusters the coordinate axis is drawn for each cluster.